5+ model PSS : 2349 Prod.Type:FTP pp.1–5(col.fig.:NIL) ED:SreejaGA PAGN:NMN SCAN:

ARTICLE IN PRESS

Available online at www.sciencedirect.com
ScienceDirect
Planetary and Space Science ▮ (▮▮▮▮) ▮▮▮–▮▮▮
Planetary and Space Science
www.elsevier.com/locate/pss

Initial Venus Express magnetic field observations of the Venus bow shock location at solar minimum

T.L. Zhang[a,g,*], M. Delva[a], W. Baumjohann[a], M. Volwerk[a], C.T. Russell[b], S. Barabash[c], M. Balikhin[d], S. Pope[d], K.-H. Glassmeier[e], K. Kudela[f], C. Wang[g], Z. Vörös[a], W. Zambelli[a]

[a]*Space Research Institute, Austrian Academy of Sciences, 8042 Graz, Austria*
[b]*IGPP, University of California, Los Angels, USA*
[c]*Swedish Institute of Space Physics, Kiruna, Sweden*
[d]*University of Sheffield, Sheffield, UK*
[e]*Institut für Geophysik und Extraterrestrische Physik, TU Braunschweig, Germany*
[f]*Institute of Experimental Physics, Slovakia Academy of Sciences, Kosice, Slovakia*
[g]*State Key Laboratory of Space Weather, Chinese Academy of Sciences, China*

Received 18 July 2007; accepted 2 September 2007

Abstract

In this study, magnetic field measurements obtained by the Venus Express spacecraft are used to determine the bow shock position at solar minimum. The best fit of bow shock location from solar zenith angle 20–120° gives a terminator bow shock location of 2.14 R_V (1 $R_V = 6052$ km) which is 1600 km closer to Venus than the 2.40 R_V determined during solar maximum conditions, a clear indication of the solar cycle variation of the Venus bow shock location. The best fit to the subsolar bow shock is 1.32 R_V, with the bow shock completely detached. Finally, a global bow shock model at solar minimum is constructed based on our best-fit empirical bow shock in the sunlit hemisphere and an asymptotic limit of the distant bow shock which is a Mach cone under typical Mach number of 5.5 at solar minimum. We also describe our approach to making the measurements and processing the data in a challenging magnetic cleanliness environment. An initial evaluation of the accuracy of measurements shows that the data are of a quality comparable to magnetic field measurements made onboard magnetically clean spacecraft.

Q1 *Keywords:* ■; ■; ■

1. Introduction

The Venus Express mission, launched on November 9, 2005 from Baikonur, is the first European mission to Venus (Titov et al., 2006). It reached Venus about 5 months later, on April 11, 2006, when a delicate manoeuvre injected it into a highly elliptical polar orbit with a period of 24 h around the planet. Among other instruments, it carries a magnetometer to investigate the Venus plasma environment (Zhang et al., 2006).

Due to the lack of an intrinsic magnetic field, the interaction of the solar wind with Venus is quite different from that at the Earth in many aspects. In particular, the solar wind interaction at Venus is strongly affected by solar activity. The bow shock heats the solar wind and deflects it around the planetary obstacle as at the Earth. Other than in the region of backstreaming particles, the bow shock provides the earliest evidence to the solar wind of the approaching obstacle to the flow. Thus, the location of the planetary bow shock provides information on the nature of the planetary obstacle.

Many previous researchers have examined the response of the bow shock position to various external solar wind conditions. By classifying the PVO shock crossings in terms of solar wind plasma parameters, the effects of solar wind dynamic pressure, Mach numbers, interplanetary magnetic field (IMF) orientation, and solar cycle on the bow shock

*Corresponding author at: Space Research Institute, Austrian Academy of Sciences, 8042 Graz, Austria.
E-mail address: Tielong.Zhang@oeaw.ac.at (T.L. Zhang).

0032-0633/$ - see front matter © 2008 Published by Elsevier Ltd.
doi:10.1016/j.pss.2007.09.012

have been deduced (cf., Slavin et al., 1980; Russell et al., 1988; Zhang et al., 1990, 2004). Nevertheless, due to the orbital bias of PVO, the subsolar bow shock locations are not well defined and the best-fit technique of the bow shock location determination is only valid for the terminator shock. In this aspect, the orbit of the Venus Express is more suitable to study the subsolar bow shock at solar minimum than that of PVO. Fig. 1 shows two typical orbits of the Venus Express spacecraft. The bow shock position depicted has been derived from an earlier bow shock model. As we can see, the trajectories of the spacecraft cross the bow shock at a highly inclined angle. Thus, multiple crossings rarely occur and the bow shock crossings are well defined. Therefore, we may simply construct the best fit to the locations of the bow shock crossings, to obtain the average bow shock position. Here we report the preliminary results from the magnetic field measurements of the Venus bow shock at solar minimum.

2. Instrumentation and data reduction

The Venus Express magnetometer consists of two triaxial fluxgate sensors, one is mounted to the tip of a 1-m deployable boom, provided by the magnetometer team as a part of the overall instrument, whereas the other is directly attached to the spacecraft. Since no efforts were made to produce a magnetically clean spacecraft and payload due to the tight schedule and budget, the measurements returned by the magnetometer contain a significant amount of spacecraft generated field effects. Under nominal operation, thousands of spacecraft generated disturbance events are recorded per day. The outboard sensor typically experiences stray fields of approximately 200 nT and the inboard sensor about 2000–6000 nT. Thus, the data processing and cleaning tasks are formidable and unprecendented.

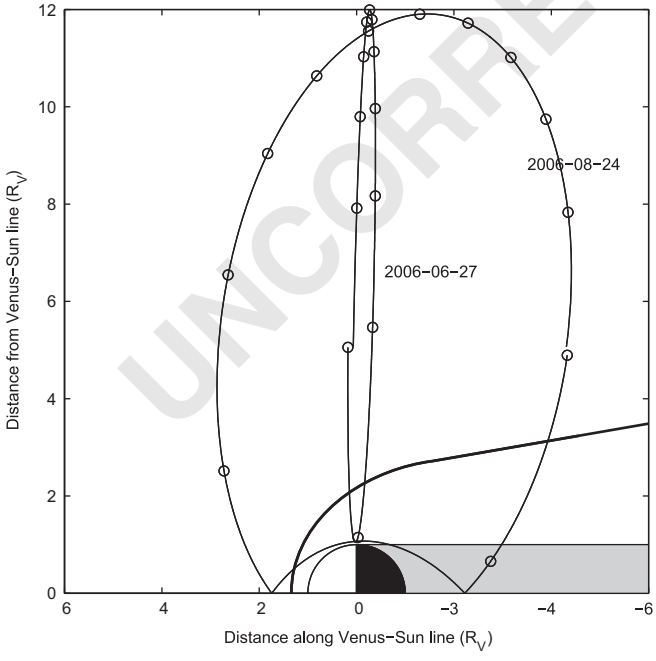

Fig. 1. Typical orbits of the Venus Express spacecraft.

The instrument has been carefully designed to cope with this great challenge of a "dirty" spacecraft with a large dynamic range between up to ±8388.6 nT and a high digital resolution. In addition, an artificial magnetic field of ±10,000 nT can be applied to each sensor for compensation of any disturbing spacecraft stray field. In operation, the default range for the outboard sensor is set to ±262 nT with a resolution of 8 pT. The default range for the inboard sensor is ±524 nT. By selecting such relatively small default dynamic ranges, we are able to obtain good data resolution, but have the risk of saturation of the inboard sensor from time to time. Typically, the inboard sensor will be saturated about two to four times per day due to the switch on/off of antenna transmissions and the solar array driving mechanism (SADM) changing the angle of the solar panels. Although autocompensation immediately follows, we lose about 2–4 min of data per day when the inboard sensor saturation occurs. Nevertheless, we feel that the trade-off between range and continuous coverage is justified by the higher resolution data obtained.

Based on these dual-sensor measurements (Ness et al., 1971), we can separate the ambient natural magnetic field from the spacecraft generated interference. A novel software procedure has been developed to detect all the disturbances using the difference of the inboard and outboard sensor measurements as the input to a system using pattern recognization and fuzzy logic algorithms. Typically more than 1500 events per day are detected in the field measurement data. Out of these events several hundred make a significant contribution to the field measured at the outboard sensor and have to be removed.

First we use the difference of the inboard and outboard measurements, in combination with spacecraft housekeeping data and pattern recognition techniques, to categorize all of the disturbances. The identified disturbances which could affect the data quality are the: (1) solar array driving mechanism changes; (2) antenna transmission effects; (3) periodic changes; (4) reaction wheel effects; and (5) slow thermal drift.

Then a heuristic approach is applied to model and to determine the magnitudes and the variations of each kind of disturbance under the mantra of "model the effects, not the sources". In other words, we do not attempt to determine the cause of each disturbance and we do not explicitly model any of the sources. Instead we only determine the effect of the disturbance on the outboard sensor measurements. Automatic data cleaning software is developed to remove all identified disturbances and we will describe the algorithm elsewhere in detail. Finally, a state-of-the-art offset determination algorithm is applied to remove the large strayfield (Schwarzl et al., 2007). At this stage, it is fair to say that the accuracy of the absolute field is ~1 nT, and the accuracy of the variable field is much

Please cite this article as: Zhang, T.L., et al., Initial Venus Express magnetic field observations of the Venus bow shock location at solar.... Planet. Space Sci. (2008), doi:10.1016/j.pss.2007.09.012

better than 0.1 nT. Thus, the data are of a quality comparable to magnetic field measurements made onboard magnetically clean spacecraft.

3. Bow shock observations

In order to determine the location of the bow shock, we examined the standard magnetic field data at 4-s resolution which is averaged from the 1 and 32 Hz data telemetered from the spacecraft. As illustrated by a typical orbit in Fig. 2, the spacecraft spends the majority of its orbit, about 22–23 h, in the solar wind. The inbound and outbound bow shock crossings occur within an interval of 1–2 h around pericenter. The data are shown in Venus Solar Orbital (VSO) coordinates where the X-axis points from Venus to the Sun, the Y-axis is opposite to the Venus orbital motion and Z-axis is northward.

In Fig. 3, we show the bow shock crossings during April–August 2006. Altogether, we have obtained 147 clear crossings. Due to the orbital geometry of Venus Express, multiple shock crossings over the sunlit hemisphere rarely occur. The shock locations were then fit using a conic section curve with its focus at the center of the planet. The equation for the conic section is

$$R = \frac{L}{1 + \varepsilon \cos(\mathrm{SZA})},$$

where R is the observed bow shock planetocentric distance,

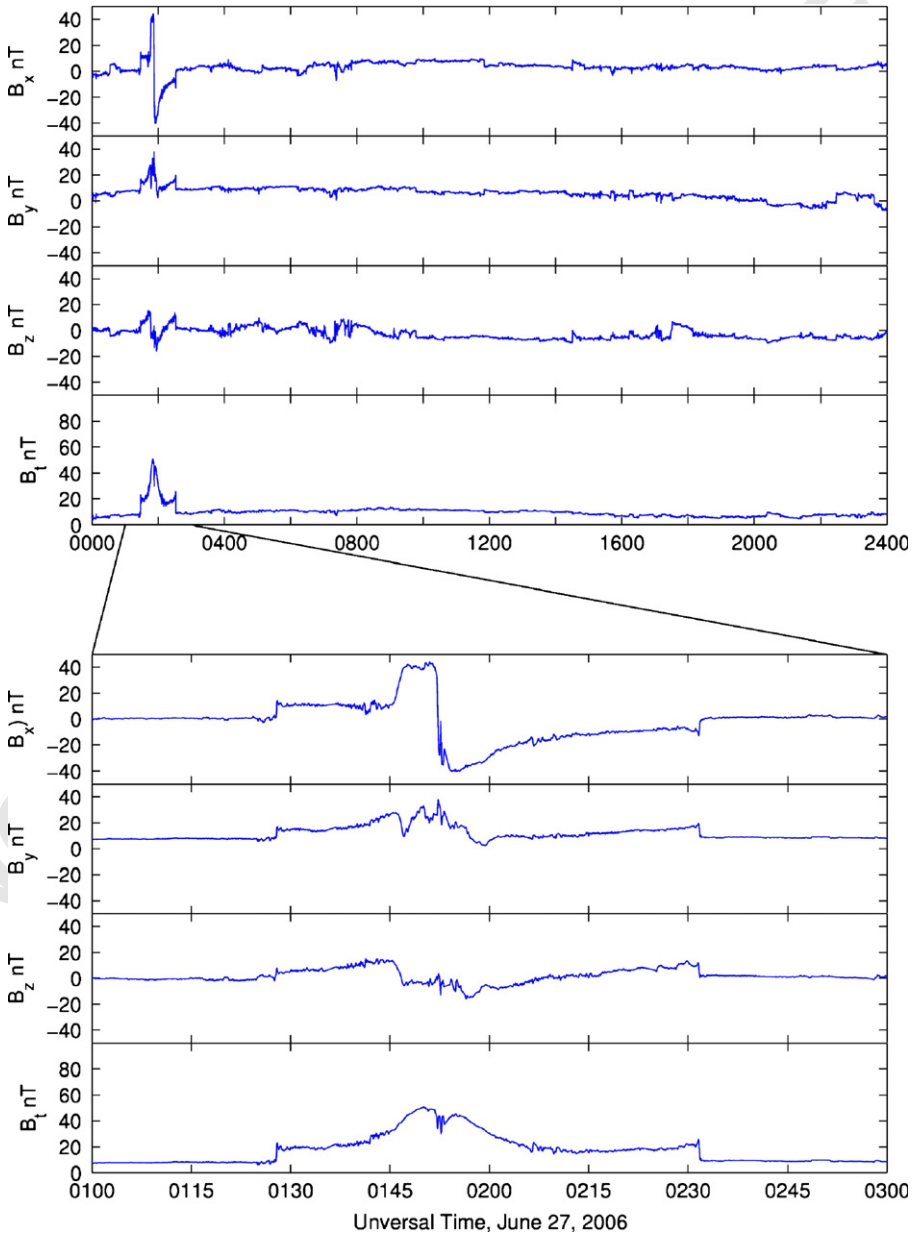

Fig. 2. Magnetic field measurements during a typical orbit where the spacecraft spends the majority of its orbit in the solar wind.

Please cite this article as: Zhang, T.L., et al., Initial Venus Express magnetic field observations of the Venus bow shock location at solar.... Planet. Space Sci. (2008), doi:10.1016/j.pss.2007.09.012

L is the terminator crossing, ε is the eccentricity, and SZA is the solar zenith angle.

The best fit for the bow shock location from SZA 20° to 120° gives an eccentricity of $\varepsilon = 0.621$ and a terminator bow shock location of 2.14 R_V, which is slightly smaller than the 2.40 R_V at solar maximum (Russell et al., 1988). The best fit returns a subsolar bow shock distance of 1.32 R_V.

4. Discussion

The size of a bow shock is largely determined by the size of the planetary obstacle, but also by how completely the planet deflects the solar wind. A study of the bow shock gives insight into the nature of the interaction of the solar wind with the planetary obstacle. The Venus bow shock was well studied by PVO over a solar cycle. However, because of the orbital bias of PVO, the subsolar bow shock locations were not well determined. The orbit of Venus Express is more suitable to study the subsolar bow shock than that of PVO.

In this paper, we determine the dayside bow shock location and shape by best fitting well-identified shock crossings using a conic section with the focus at the center of the planet. We note that the obtained shock model is only valid over a limited SZA range, about 0° to ~120°, since an eccentricity of 0.621 implies that the best fit is an ellipse that closes behind the planet. For the distant bow shock, i.e., for SZA larger than ~120°, the bow shock is best represented by an asymptotic shock cone, i.e., a Mach cone to be determined by the prevailing solar wind conditions (Slavin et al., 1984). Under solar minimum condition, the magnetosonic Mach number is about 5.5 and the Mach cone angle is 10.5°. Thus, to zeroth order, a global bow shock model at solar minimum can be constructed by superimposing a best-fit dayside bow shock model of $\varepsilon = 0.621$ and an asymptotic shock cone of 10.5° (Fig. 4):

$$r = \frac{2.14}{1 + 0.621\cos(\mathrm{SZA})} \quad \text{for SZA} \leqslant 117^\circ$$

$$r = \frac{2.364}{\sin(\mathrm{SZA} + 10.5^\circ)} \quad \text{for SZA} > 117^\circ$$

It is apparent that the location of the bow shock is highly variable. Part of the observed variation of the shock position can be attributed to EUV variation and part to short-term effects, such as the variation of solar wind Mach number and IMF orientation. Nevertheless, even when we used our bow shock shape to extrapolate the closest locations of the bow shock to the subsolar point, the bow shock was still well above the subsolar obstacle height. Thus, the bow shock is completedly detached based on our investigation so far, which answers the question posed long ago by Russell (1977) on whether the Venusian bow shock is detached or not at solar minimum.

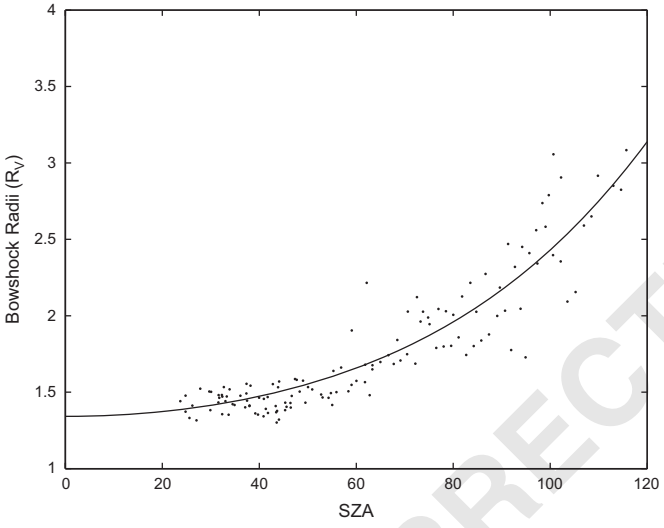

Fig. 3. Bow shock crossings during April–August 2006. The solid line is the best fit of the shock crossings.

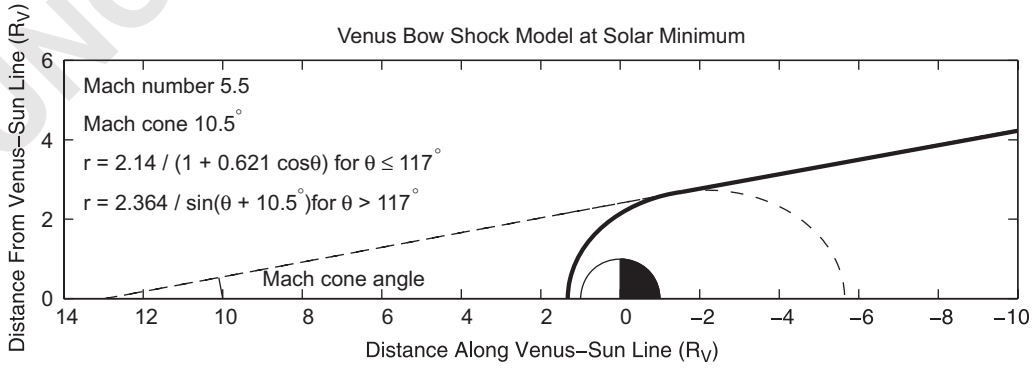

Fig. 4. Venus bow shock model at solar minimum based on the empirical best fit of the bow shock crossings and an asymptotic shock cone determined by an average Mach number of 5.5 at solar minimum. The tangent point of the Mach cone and the ellipsoid is at 117°.

Please cite this article as: Zhang, T.L., et al., Initial Venus Express magnetic field observations of the Venus bow shock location at solar.... Planet. Space Sci. (2008), doi:10.1016/j.pss.2007.09.012

Acknowledgments

The work at UCLA was supported by the National Aeronautics and Space Administration under research grant NNG06GC62G. The work in Slovakia was supported by Slovak Research and Development Agency under the contract no. APVV-51-053805. The work in China was supported by NNSFC project 40628003.

References

Ness, N.F., Behannon, K.W., Lepping, R.P., Schatten, K.H., 1971. Use of two magnetometers for magnetic field measurements on a spacecraft. J. Geophys. Res. 76, 3565–3573.

Russell, C.T., 1977. The Venus bow shock: detached or attached. J. Geophys. Res. 82, 625–631.

Russell, C.T., Chou, E., Luhmann, J.G., Gazis, P., Brace, L.H., Hoegy, W.R., 1988. Solar and interplanetary control of the location of the Venus bow shock. J. Geophys. Res. 93, 5461–5469.

Schwarzl, H., et al., 2007. An optimal approach to finding magnetometer zero levels in the interplanetary magnetic field. J. Geophys. Res., to be submitted.

Slavin, J.A., Elphic, R.C., Russell, C.T., Scarff, L., Wolfe, J.H., Mihalov, J.D., Intriligator, D.S., Brace, L.H., Taylor Jr., H.A., Daniell Jr., R.E., 1980. The solar wind interaction with Venus: Pioneer Venus observations of bow shock location and structure. J. Geophys. Res. 85, 7625–7641.

Slavin, J.A., Holzer, R.E., Spreiter, J.R., Stahara, S.S., 1984. Planetary Mach cones: theory and observation. J. Geophys. Res. 89, 2708–2714.

Titov, D.V., Svedhem, H., Koschny, D., Hoofs, R., Barabash, S., Zhang, T.L., Formisano, V., Bertaux, J.-L., Nevejans, D., Korablev, O., Häusler, B., Pätzold, M., Drossart, P., Piccioni, G., Markiewicz, W., Merritt, D., Witasse, O., Accommazzo, A., Sweeney, M., Trillard, D., Janvier, M., Clochet, A., 2006. Venus Express science planning. Planet. Space Sci. 54, 1279–1297.

Zhang, T.L., Luhmann, J.G., Russell, C.T., 1990. The solar cycle dependence of the location and shape of the Venus bow shock. J. Geophys. Res. 95, 14961–14967.

Zhang, T.L., Khurana, K.K., Russell, C.T., Kivelson, M.G., Nakamura, R., Baumjohann, W., 2004. On the Venus bow shock compressibility. Adv. Space Res. 33, 1920–1923.

Zhang, T.L., et al., 2006. Magnetic field investigation of the Venus plasma environment: expected new results. Planet. Space Sci. 54, 1336–1343.

Please cite this article as: Zhang, T.L., et al., Initial Venus Express magnetic field observations of the Venus bow shock location at solar.... Planet. Space Sci. (2008), doi:10.1016/j.pss.2007.09.012